AIAA JOURNAL
Vol. 36, No. 8, August 1998

# Transient Response Analysis of Nonlinear Modally Coupled Structural Dynamics Equations of Motion

Joseph A. Fromme*
*Morrison, Colorado 80465*
and
Michael A. Golberg†
*Las Vegas, Nevada 89119*

**The solution of the structural dynamics matrix differential equations of motion in the presence of general structural damping, aerodynamic stiffness and damping, and nonlinear generalized forces is discussed. An intuitive and easy-to-use method of Picard iteration by Dawson is shown to provide exponential convergence to the exact solution of quasilinear second-order matrix differential equations with general modal coupling, and the first mathematical proof of convergence is presented. It is demonstrated, for the special case of general structural damping without aerodynamic forces but with forcing functions that depend only on time, that the method of Picard iteration agrees to within machine accuracy with the method of linear modal velocity of Henkel and Mar. Thomson's coupled damping problem is solved using both methods and percent errors resulting from ignoring modal coupling are quantified. Possible areas of future research are discussed.**

## I. Introduction

DIFFERENTIAL equations with modal coupling arise in a wide variety of problems in science and engineering. Therefore it is of great importance to be able to integrate them economically and accurately. In structural dynamics, the normal mode transformation eliminates mass and stiffness coupling, but modal coupling may persist through structural damping or the system forcing functions. Examples may be found in structures with fluid–solid interaction, such as flight vehicles subject to aerodynamic forces, viscoelastic isolation systems, offshore platforms with fluid damping, buildings on highly damped soil, and structures with discrete dampers.[1]

If structural damping is negligible and the forcing functions do not depend upon displacements or velocities, then the normal mode transformation simultaneously diagonalizes the mass and stiffness matrices, leaving an uncoupled system of ordinary differential equations that can be integrated analytically by elementary methods. However, for damped systems, the same modal coordinate transformation, in general, will result in a coupled modal damping matrix, thus complicating the computational effort.

Although generally small and not as well understood as mass and stiffness properties, structural damping can affect dynamic loads significantly.[2,3] In practice, damping matrices are seldom computed from first principles but are instead estimated after the fact, not always with the benefit of a modal survey. When modal survey tests of complex aerospace structures are conducted, it is usually at the component level, so that coupled system modal damping matrices computed from possibly test-verified component models almost certainly will be coupled. Until recently, modal surveys have measured only diagonal elements of the modal damping matrix, leaving unanswered the question of off-diagonal terms. However, in 1993, Balmès and Crawley[4] achieved the first successful experimental characterization of a full modal damping matrix for a modestly complex structure. This important contribution will improve the physical understanding of structural damping. Hence it becomes even more important in a concurrent engineering sense to be able to analyze arbitrary damping effects quickly and accurately.

In 1957, Foss[5] at the Massachusetts Institute of Technology proved for a damped linear elastic system with time-dependent forces that the second-order differential equations of motion can be recast into state space with twice as many first-order differential equations possessing complex eigenvalues and eigenvectors. However, the use of Foss's method has been limited in structural dynamics, perhaps in part because most loads analysis programs remain formulated in the real domain.

Approximate integration methods such as Runge–Kutta and Newmark–Beta can be employed to integrate coupled systems of equations of motion, but these direct methods are relatively slow and expensive and can pose time-step instability problems. However, the use of modal coordinates, if it can be made to work, as we show, offers several advantages. Frequencies and modes provide indispensable physical insight into the dynamical properties of the structure, the mass and stiffness matrices become uncoupled thereby simplifying the computations, modal analysis opens the door to frequency limited modal truncation simplifying the computations further, and computations are fast, accurate, and unconditionally stable.

Historically, to simplify the computations, it has been common practice in structural dynamics to neglect off-diagonal terms of the coupled system modal damping matrix for the purpose of coupled loads analysis, and sometimes to neglect structural damping altogether. However, it is well known that even small amounts of structural damping can significantly affect dynamic loads, generally (but not uniformly) conservatively because energy is being dissipated. Commonly, diagonal modal damping is assigned, as if it were so, as a function of frequency. Modal damping values for aerospace structures typically range from about 1 to 3% of critical, with exceptions for lightly damped slosh modes and highly damped components such as actuators. A common variation is to compute the coupled system modal damping matrix correctly from the component matrices, but then to simply ignore the off-diagonal elements. However, by transforming a presumptively diagonalized modal damping matrix back to the original coordinates, Henkel and Mar[3] showed reductio ad absurdum that diagonalizing the modal damping matrix is erroneous because it results in physically impossible damping across component noninterface degrees of freedom. Further, it has been shown for the Space Shuttle and Titan IV vehicles that significant errors in coupled payload loads result from neglecting off-diagonal elements of the coupled modal damping matrix.[2,3,6] Using an ingenious approximation, which we shall call the linear modal velocity method, that the modal velocities are linear between time steps, Henkel and Mar[3] found that Space Shuttle payload load predictions using diagonalized modal damping were inaccurate and sometimes

Presented as Paper 97-1280 at the AIAA/ASME/ASCE/AHS/ASC 38th Structures, Structural Dynamics, and Materials Conference, Kissimmee, FL, April 7–10, 1997; received Oct. 24, 1997; revision received Feb. 6, 1998; accepted for publication Feb. 10, 1998. 

*Consultant, 10455 South Crystal Drive. Senior Member AIAA.
†Consultant, 2025 University Circle.

nonconservative. Chapman[6] reported similar results for both Shuttle and Titan IV payload loads, and presented a simple two-degree-of-freedom example with equal frequencies but different modal damping ratios that explicitly demonstrates possible errors due to neglecting off-diagonal damping. Chapman validated the linear modal velocity method against a variety of direct integration methods, specifically a modified Newmark–Beta algorithm, a fourth-order fixed-step Runge–Kutta, a fifth-order variable-step Runge–Kutta–Fehlberg, and a twelfth-order Adams predictor-corrector. He found that direct integration methods required approximately four to eight times as much computer time to achieve the same accuracy. Using an unpublished iteration technique, Dawson found similar results for a Titan IV payload,[7] as did Fromme and Stroman, using Dawson's method, for the Titan IV indicator payloads.[2] Although all investigators reported rapid convergence, the accuracy and convergence of computational methods used for solving modally coupled equations of motion were not fully understood at that time.

This paper shows that the form of Picard iteration used by Dawson guarantees exponential convergence to the exact solution of modally coupled nonlinear differential equations as long as the generalized forces are Lipschitz continuous (see Definition 3) in displacements and velocities. The practical advantage of exponential convergence is that the number of decimals of accuracy is proportional to the number of iterations. Consequently, arbitrary accuracy can be achieved with minimal computing time, and machine accuracy can be achieved with a fairly small number of iterations. This makes practical the automatic machine-accurate solution of large systems of coupled quasilinear second-order ordinary differential equations where the option of including modal coupling is transparent and reduced to a matter of input data (yes/no).

## II. Formulation

Following common practice in mathematics and mechanics, denote vectors and tensors in boldface and scalars in standard face. Consider the quasilinear second-order matrix initial value problem

$$\boldsymbol{M}\ddot{\boldsymbol{u}} + \boldsymbol{C}\dot{\boldsymbol{u}} + \boldsymbol{K}\boldsymbol{u} = \boldsymbol{F}(t, \boldsymbol{u}, \dot{\boldsymbol{u}}), \qquad \boldsymbol{u}(t_0) = \boldsymbol{u}_0, \qquad \dot{\boldsymbol{u}}(t_0) = \dot{\boldsymbol{u}}_0 \tag{1a}$$

where $\boldsymbol{u}$ is the coupled system vector representing physical displacements or generalized coordinates, $\boldsymbol{u}_0$ and $\dot{\boldsymbol{u}}_0$ are initial conditions, and $\boldsymbol{F}$ is the corresponding applied generalized force vector. For structural dynamics problems, $\boldsymbol{M}$, $\boldsymbol{C}$, and $\boldsymbol{K}$ are the coupled-system mass, damping, and stiffness matrices, respectively. In general, all are real symmetric positive-semidefinite matrices, and $\boldsymbol{M}$ is strictly positive definite. In special cases in which the structure is grounded, the stiffness matrix is also positive definite, though the same statement cannot be made for the damping matrix. For systems with linearized aerodynamic forces, an equivalent variation of Eq. (1a) is

$$\boldsymbol{M}\ddot{\boldsymbol{u}} + \boldsymbol{C}\dot{\boldsymbol{u}} + \boldsymbol{K}\boldsymbol{u} = \boldsymbol{F}(t, \boldsymbol{u}, \dot{\boldsymbol{u}}) - \boldsymbol{C}_A\dot{\boldsymbol{u}} - \boldsymbol{K}_A\boldsymbol{u}$$
$$\boldsymbol{u}(t_0) = \boldsymbol{u}_0, \qquad \dot{\boldsymbol{u}}(t_0) = \dot{\boldsymbol{u}}_0 \tag{1b}$$

where the terms containing the aerodynamic damping and stiffness matrices $\boldsymbol{C}_A$ and $\boldsymbol{K}_A$ represent the linearized dynamic angle-of-attack contributions to generalized aerodynamic forces due to lateral velocity and to streamwise rotational degrees of freedom. In either case, transform the original coordinates $\boldsymbol{u}$ to modal coordinates $\boldsymbol{q}$,

$$\boldsymbol{u} = \boldsymbol{\Phi}\boldsymbol{q} \tag{2a}$$

where $\boldsymbol{\Phi}$ is the mass-normalized modal matrix satisfying

$$\boldsymbol{\Phi}^T\boldsymbol{M}\boldsymbol{\Phi} = \boldsymbol{I}, \qquad \boldsymbol{\Phi}^T\boldsymbol{K}\boldsymbol{\Phi} = \boldsymbol{\omega}^2 \tag{2b}$$

where $\boldsymbol{I}$ and $\boldsymbol{\omega}^2$ are the identity matrix and diagonal matrix of free-vibration undamped natural frequencies squared, respectively. Equations (2) transform Eq. (1) into the quasilinear, pseudo-uncoupled modal differential equation of motion

$$\ddot{\boldsymbol{q}} + 2\boldsymbol{\zeta}\boldsymbol{\omega}\dot{\boldsymbol{q}} + \boldsymbol{\omega}^2\boldsymbol{q} = \boldsymbol{Q}(t, \boldsymbol{q}, \dot{\boldsymbol{q}}) - \boldsymbol{X}\dot{\boldsymbol{q}}$$
$$\boldsymbol{q}(t_0) = \boldsymbol{q}_0, \qquad \dot{\boldsymbol{q}}(t_0) = \dot{\boldsymbol{q}}_0 \tag{3a}$$

where the left-hand side is identically uncoupled, where

$$2\boldsymbol{\zeta}\boldsymbol{\omega} = \operatorname{diag}(\boldsymbol{\Phi}^T\boldsymbol{C}\boldsymbol{\Phi}), \qquad \boldsymbol{X} = \operatorname{nondiag}(\boldsymbol{\Phi}^T\boldsymbol{C}\boldsymbol{\Phi})$$
$$\boldsymbol{Q} = \boldsymbol{\Phi}^T\boldsymbol{F}, \qquad \boldsymbol{q}_0 = \boldsymbol{\Phi}^{-1}\boldsymbol{u}_0, \qquad \dot{\boldsymbol{q}}_0 = \boldsymbol{\Phi}^{-1}\dot{\boldsymbol{u}}_0 \tag{3b}$$

where $\boldsymbol{\zeta}$ is the diagonal matrix of modal damping ratios and $\boldsymbol{X}$ is the modal cross-coupling damping matrix. In general, $\boldsymbol{X} \neq \boldsymbol{0}$. Although tempting, generalized proportional damping, where

$$\boldsymbol{C} = a_1\boldsymbol{M} + a_2\boldsymbol{K} + a_3\boldsymbol{K}\boldsymbol{M}^{-1}\boldsymbol{K} + a_4\boldsymbol{K}\boldsymbol{M}^{-1}\boldsymbol{K}\boldsymbol{M}^{-1}\boldsymbol{K} + \cdots$$

giving

$$\boldsymbol{\Phi}^T\boldsymbol{C}\boldsymbol{\Phi} = 2\boldsymbol{\zeta}\boldsymbol{\omega} = a_1\boldsymbol{I} + a_2\boldsymbol{\omega}^2 + a_3\boldsymbol{\omega}^4 + \cdots, \qquad \boldsymbol{X} = \boldsymbol{0}$$

does not represent physically general damping and cannot avoid modal coupling arising from the forcing functions. Proportional damping is a mathematical nicety of quite limited practical value and is seldom even approximated in real-world physical systems.

However, if the modal damping matrix is diagonal and the generalized forces do not depend upon displacement and velocity, then Eq. (3a) reduces to the uncoupled system of elementary linear second-order differential equations with initial conditions,

$$\ddot{\boldsymbol{q}} + 2\boldsymbol{\zeta}\boldsymbol{\omega}\dot{\boldsymbol{q}} + \boldsymbol{\omega}^2\boldsymbol{q} = \boldsymbol{Q}(t), \qquad \boldsymbol{q}(t_0) = \boldsymbol{q}_0, \qquad \dot{\boldsymbol{q}}(t_0) = \dot{\boldsymbol{q}}_0 \tag{4a}$$

which for each mode $\alpha$ has the analytic solution, valid for all damping ratios,

$$q_\alpha(t) = \exp[-\zeta_\alpha\omega_\alpha(t - t_0)]\Big\{q_{\alpha_0}[\xi_S(t - t_0) + \zeta_\alpha\omega_\alpha\xi_A(t - t_0)] + \dot{q}_{\alpha_0}\xi_A(t - t_0)\Big\} + \int_{t_0}^{t} \exp[-\zeta_\alpha\omega_\alpha(t - \tau)]\xi_A(t - \tau)\,Q_\alpha(\tau)\,\mathrm{d}\tau \tag{4b}$$

based on Laplace transforms,[8] where $\xi_S$ and $\xi_A$ are symmetric and antisymmetric fundamental solutions to the homogeneous differential equation given by

$$\xi_S(t) = \begin{cases} \cos(\bar{\omega}_\alpha t) & \text{if} \quad \omega_\alpha > 0 \quad \text{and} \quad 0 \le \zeta_\alpha < 1 \\ 1 & \text{if} \quad \zeta_\alpha = 1 \quad \text{or} \quad \omega_\alpha = 0 \\ \cosh(\bar{\omega}_\alpha t) & \text{if} \quad \omega_\alpha > 0 \quad \text{and} \quad \zeta_\alpha > 1 \end{cases} \tag{4c}$$

$$\xi_A(t) = \begin{cases} (1/\bar{\omega}_\alpha)\sin(\bar{\omega}_\alpha t) & \text{if} \quad \omega_\alpha > 0 \quad \text{and} \quad 0 \le \zeta_\alpha < 1 \\ t & \text{if} \quad \zeta_\alpha = 1 \quad \text{or} \quad \omega_\alpha = 0 \\ (1/\bar{\omega}_\alpha)\sinh(\bar{\omega}_\alpha t) & \text{if} \quad \omega_\alpha > 0 \quad \text{and} \quad \zeta_\alpha > 1 \end{cases}$$

where

$$\bar{\omega}_\alpha = \omega_\alpha\sqrt{|1 - \zeta_\alpha^2|}, \qquad \omega_\alpha \ge 0, \qquad \zeta_\alpha \ge 0 \tag{4d}$$

The fundamental solutions apply to rigid-body as well as flexible modes, are frequency and damping dependent, and change type from trigonometric to hyperbolic as the modal damping ratios vary from subcritical to supercritical. For future use, we note that their first derivatives satisfy the pairwise first-order equations

$$\dot{\xi}_S = -\omega_\alpha^2(1 - \zeta_\alpha^2)\xi_A, \qquad \dot{\xi}_A = \xi_S \tag{4e}$$

The convolution integral in Eq. (4b) represents that portion of the solution due to the applied forcing function but requires knowledge of the forcing function at all intermediate values of time and consequently is computationally incomplete as it stands. In actual practice, forcing functions often are known only at discrete points (e.g., digital flight or test data are measured at a finite sampling rate and hence are known only discretely), thus introducing an inherently unknowable error due to forcing-function discretization. Standard practice is to approximate the modal forcing function $Q_\alpha$ as a piecewise linear function of time $\hat{Q}_\alpha$ over a partition $[t_0, t_1, \ldots, t_n]$ of

discrete time points and to evaluate Eq. (4b) in closed form over the set of successive subintervals. On the $i$th subinterval $[t_i, t_{i+1}]$, the closed-form solutions $\hat{q}_\alpha$, $\dot{\hat{q}}_\alpha$, and $\ddot{\hat{q}}_\alpha$ corresponding to a piecewise linear forcing function $\hat{Q}_\alpha$ can be shown to be linear combinations of the initial values of displacement and velocity and of the initial and final values of the forcing function,

$$\begin{aligned}
\hat{q}_\alpha(t) &= U_\alpha(t-t_i)\hat{q}_\alpha(t_i) + V_\alpha(t-t_i)\dot{\hat{q}}_\alpha(t_i) \\
&\quad + G_\alpha(t-t_i)\hat{Q}_\alpha(t_i) + H_\alpha(t-t_i)\hat{Q}_\alpha(t_{i+1}) \\
\dot{\hat{q}}_\alpha(t) &= \dot{U}_\alpha(t-t_i)\hat{q}_\alpha(t_i) + \dot{V}_\alpha(t-t_i)\dot{\hat{q}}_\alpha(t_i) \\
&\quad + \dot{G}_\alpha(t-t_i)\hat{Q}_\alpha(t_i) + \dot{H}_\alpha(t-t_i)\hat{Q}_\alpha(t_{i+1}) \\
\ddot{\hat{q}}_\alpha(t) &= -2\zeta_\alpha\omega_\alpha\dot{\hat{q}}_\alpha(t) - \omega_\alpha^2\hat{q}_\alpha(t) + \hat{Q}_\alpha(t)
\end{aligned} \tag{5a}$$

where

$$\begin{aligned}
U_\alpha(t) &= \exp(-\zeta_\alpha\omega_\alpha t)[\xi_S(t) + \zeta_\alpha\omega_\alpha\xi_A(t)] \\
V_\alpha(t) &= \exp(-\zeta_\alpha\omega_\alpha t)\xi_A(t) \\
\dot{U}_\alpha(t) &= -\omega_\alpha^2\exp(-\zeta_\alpha\omega_\alpha t)\xi_A(t) \\
\dot{V}_\alpha(t) &= \exp(-\zeta_\alpha\omega_\alpha t)[\xi_S(t) - \zeta_\alpha\omega_\alpha\xi_A(t)]
\end{aligned} \tag{5b}$$

$$G_\alpha(t) = A_\alpha(t) - B_\alpha(t)/(t_{i+1}-t_i), \qquad H_\alpha(t) = B_\alpha(t)/(t_{i+1}-t_i) \tag{5c}$$

$$\dot{G}_\alpha(t) = \dot{A}_\alpha(t) - \dot{B}_\alpha(t)/(t_{i+1}-t_i), \qquad \dot{H}_\alpha(t) = \dot{B}_\alpha(t)/(t_{i+1}-t_i)$$

$$A_\alpha(t) = \begin{cases} \{1 - \exp(-\zeta_\alpha\omega_\alpha t)[\xi_S(t) + \zeta_\alpha\omega_\alpha\xi_A(t)]\}/\omega_\alpha^2 & \text{if } \omega_\alpha > 0 \text{ and } \zeta_\alpha \neq 1 \\ [1 - \exp(-\zeta_\alpha\omega_\alpha t)(1 + \zeta_\alpha\omega_\alpha t)]/\omega_\alpha^2 & \text{if } \omega_\alpha > 0 \text{ and } \zeta_\alpha = 1 \\ t^2/2 & \text{if } \omega_\alpha = 0 \text{ and } \zeta_\alpha = 0 \end{cases} \tag{5d}$$

$$\dot{A}_\alpha(t) = \begin{cases} \exp(-\zeta_\alpha\omega_\alpha t)\xi_A(t) & \text{if } \omega_\alpha > 0 \text{ and } \zeta_\alpha \neq 1 \\ \exp(-\zeta_\alpha\omega_\alpha t)t & \text{if } \omega_\alpha > 0 \text{ and } \zeta_\alpha = 1 \\ t & \text{if } \omega_\alpha = 0 \text{ and } \zeta_\alpha = 0 \end{cases} \tag{5e}$$

$$B_\alpha(t) = \begin{cases} t/\omega_\alpha^2 - \{2\zeta_\alpha\omega_\alpha - \exp(-\zeta_\alpha\omega_\alpha t)[2\zeta_\alpha\omega_\alpha\xi_S(t) + \omega_\alpha^2(2\zeta_\alpha^2 - 1)\xi_A(t)]\}/\omega_\alpha^4 & \text{if } \omega_\alpha > 0 \text{ and } \zeta_\alpha \neq 1 \\ [\exp(-\zeta_\alpha\omega_\alpha t)(2 + \zeta_\alpha\omega_\alpha t) - 2 + \zeta_\alpha\omega_\alpha t]/\omega_\alpha^3 & \text{if } \omega_\alpha > 0 \text{ and } \zeta_\alpha = 1 \\ t^3/6 & \text{if } \omega_\alpha = 0 \text{ and } \zeta_\alpha = 0 \end{cases} \tag{5f}$$

$$\dot{B}_\alpha(t) = \begin{cases} \{1 - \exp(-\zeta_\alpha\omega_\alpha t)[\xi_S(t) + \zeta_\alpha\omega_\alpha\xi_A(t)]\}/\omega_\alpha^2 & \text{if } \omega_\alpha > 0 \text{ and } \zeta_\alpha \neq 1 \\ [1 - \exp(-\zeta_\alpha\omega_\alpha t)(1 + \zeta_\alpha\omega_\alpha t)]/\omega_\alpha^2 & \text{if } \omega_\alpha > 0 \text{ and } \zeta_\alpha = 1 \\ t^2/2 & \text{if } \omega_\alpha = 0 \text{ and } \zeta_\alpha = 0 \end{cases} \tag{5g}$$

From Eqs. (5), output quantities such as bending moments, and accelerations then may be computed using standard output transformation matrix techniques. The difference between Eqs. (4b) and (5a) is precisely the error due to approximating the forcing function with a piecewise linear function and is called discretization error.

The time-honored technique of transferring inconvenient terms to the right-hand side is used in both Picard iteration and the linear modal velocity method. In the latter case, generalized forces are functions of time only, and if both the forcing function and the modal velocities in the right-hand side of Eq. (3a) are approximated by piecewise continuous linear functions of time, then the first two equations in Eqs. (5a) may be applied in matrix form and solved simultaneously for all modes, leaving only discretization error. Henkel and Mar,[3] Chapman,[6] Abdallah (Abdallah, A., Analex-NASA Lewis Research Center, Cleveland, Ohio, private communication, 1996), and others have shown that a solution at $t = t_{i+1}$ containing only discretization error is given by

$$\begin{aligned}
\dot{\hat{\boldsymbol{q}}}_{i+1} &= [\boldsymbol{I} + \dot{\boldsymbol{H}}(t_{i+1}-t_i)\boldsymbol{X}]^{-1}\{\dot{\boldsymbol{U}}(t_{i+1}-t_i)\hat{\boldsymbol{q}}_i + \dot{\boldsymbol{V}}(t_{i+1}-t_i)\dot{\hat{\boldsymbol{q}}}_i \\
&\quad + \dot{\boldsymbol{G}}(t_{i+1}-t_i)[\hat{\boldsymbol{Q}}(t_i) - \boldsymbol{X}\dot{\hat{\boldsymbol{q}}}_i] + \dot{\boldsymbol{H}}(t_{i+1}-t_i)\hat{\boldsymbol{Q}}(t_{i+1})\} \\
\hat{\boldsymbol{q}}_{i+1} &= \boldsymbol{U}(t_{i+1}-t_i)\hat{\boldsymbol{q}}_i + \boldsymbol{V}(t_{i+1}-t_i)\dot{\hat{\boldsymbol{q}}}_i + \boldsymbol{G}(t_{i+1}-t_i) \\
&\quad \times [\hat{\boldsymbol{Q}}(t_i) - \boldsymbol{X}\dot{\hat{\boldsymbol{q}}}_i] + \boldsymbol{H}(t_{i+1}-t_i)[\hat{\boldsymbol{Q}}(t_{i+1}) - \boldsymbol{X}\dot{\hat{\boldsymbol{q}}}_{i+1}] \\
\ddot{\hat{\boldsymbol{q}}}_{i+1} &= -(2\boldsymbol{\zeta}\boldsymbol{\omega} + \boldsymbol{X})\dot{\hat{\boldsymbol{q}}}_{i+1} - \boldsymbol{\omega}^2\hat{\boldsymbol{q}}_{i+1} + \hat{\boldsymbol{Q}}(t_{i+1})
\end{aligned} \tag{6}$$

where the modal components of the vectors and matrices shown in boldface type are the scalars with the same symbols in lightface type, e.g., $\hat{\boldsymbol{q}} = \{\hat{q}_\alpha\}$, $\boldsymbol{U} = \text{diag}[U_\alpha]$, etc. Equation (6) must be computed in the order shown, requires a matrix inversion with an operation count of approximately the cube of the number of retained modes, and is not an exact solution because the modal velocities in $(6)_1$ are not piecewise linear as assumed.

Picard iteration is a form of successive approximations that requires no matrix inversion. Its practical import is to solve quickly and accurately the general equations of motion (3) including the effects of aerodynamic damping and stiffness and nonlinear forcing functions of displacement and velocity. The zeroth iteration, or starting point, neglects the damping cross-coupling matrix $X$ and solves the diagonally damped modal equations. Successive iterations use the modal solution from the previous iteration on the right-hand side to approximate the effect of modal coupling during the current iteration. The practical result is that each iteration is exponentially more accurate than the preceding one, so that highly accurate solutions can be obtained with a small number of iterations. If it is desired to neglect modal coupling, Picard iteration can be stopped after the zeroth iteration. Also, existing computer programs using Eqs. (5) can be modified easily to perform Picard iteration.

## III. Discretization Error

The method of Picard iteration for solving modally coupled quasilinear equations of motion rests upon the solution to modally uncoupled linear equations. Thus, we digress briefly to formulate their error analysis. Let $\boldsymbol{f}$ be any vector function of time approximated by $\hat{\boldsymbol{f}}$. Define the absolute error, relative error, and number of decimals of accuracy, respectively, as

$$\varepsilon_f(t) = \|\hat{\boldsymbol{f}}(t) - \boldsymbol{f}(t)\|_\infty, \qquad \bar{\varepsilon}_f(t) = \|\hat{\boldsymbol{f}}(t) - \boldsymbol{f}(t)\|_\infty / \|\hat{\boldsymbol{f}}(t)\|_\infty \tag{7a}$$

$$ND_f(t) = -\log_{10}(\bar{\varepsilon}_f(t))$$

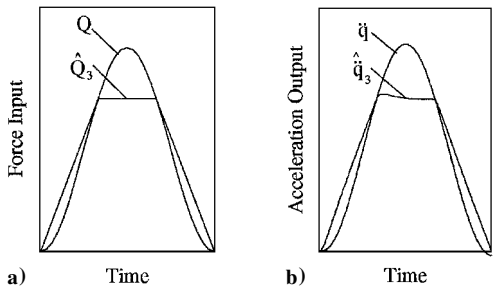


**Fig. 1 Input and output discretization errors.**

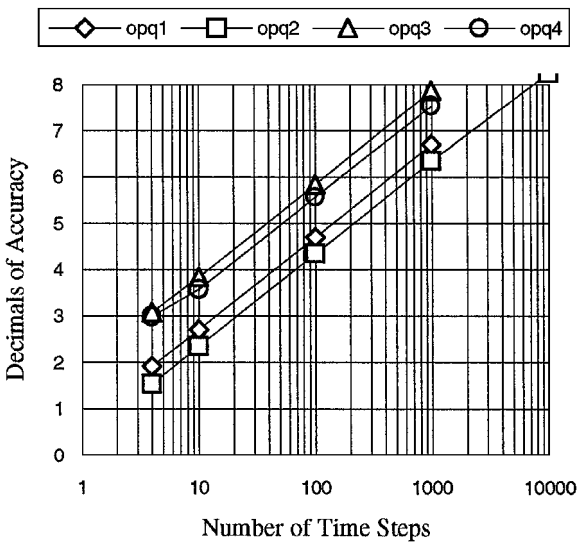


**Fig. 2 Inverse-square discretization convergence.**

where

$$\|\boldsymbol{f}(t)\|_\infty \equiv \max(|f_1(t)|, |f_2(t)|, \ldots) \tag{7b}$$

is the pointwise infinity norm of a vector function.

Figures 1 and 2 illustrate forcing function and acceleration discretization error obtained for a 1-cosine axial pulse acting on a simple two-degree-of-freedom linear system excited from rest at one node.[9] Figure 1a shows the exact forcing function $Q$ and a three-point piecewise linear approximant $\hat{Q}_3$ which is collocated at three points. Figure 1b shows the solutions for the exact acceleration $\ddot{q}$ based on $Q$ and the approximate acceleration $\hat{\ddot{q}}_3$ based on $\hat{Q}_3$, each displaying clear hereditary attributes of their corresponding parent forcing functions. For continuous forcing functions approximated by piecewise linear functions with equal time steps, it is well known that the relative error $\bar{\varepsilon}_1$ of the solution (5) is inversely proportional to the square of the number of time steps,

$$\bar{\varepsilon}_1 = c_1 \big/ n^2, \qquad ND_1 = 2\log_{10} n - \log_{10} c_1 \tag{8}$$

Thus, graphs of the number of decimals of accuracy of various output quantities vs the logarithm of the number of time steps may be expected to be a family of straight lines, all with slope of 2. Figure 2 shows the results of a computational test case verifying the expected inverse-square discretization error for four different output quantities.[9]

## IV. Picard Iteration

Picard iteration can be used to solve a variety of fixed-point equations of the form $x = f(x)$ by iteratively evaluating $x^{(k)} = f(x^{(k-1)})$ until convergence is achieved. For example, the buckling load of a fixed-pinned beam-column is governed by the fixed-point equation $\lambda = \tan\lambda$, where in terms of the elementary beam parameters, $\lambda^2 = PL^2/EI$, $P$ is buckling load, $L$ is length, $E$ is Young's modulus, and $I$ is areal moment of inertia. The $n$th root of this equation can be computed by the Picard iterations $\lambda^{(k)} = \tan^{-1}(\lambda^{(k-1)}) + n\pi$ where $\lambda^{(0)}$ is arbitrary. Exponential convergence can be obtained quickly and easily with a simple hand-held calculator. Another example is the class of nonlinear fixed-base force-displacement equations $\boldsymbol{F} = \boldsymbol{K}(\boldsymbol{u})\boldsymbol{u}$, which can be converted to a fixed-point equation and solved iteratively with $\boldsymbol{u}^{(k)} = K^{-1}(\boldsymbol{u}^{(k-1)})\,\boldsymbol{F}$. For viscoelastic trusses with kinematic nonlinearities, this particular iteration scheme has demonstrated exponential convergence and has been verified by Newton–Jacobi iteration.[10] We will show that Picard iteration can be used to solve the second-order quasilinear differential equations of structural dynamics with nonlinear modal coupling and that the error will decrease exponentially with the number of iterations.

Consider the problem of integrating Eq. (3) over the subinterval $[t_i, t_{i+1}]$. Let the zeroth iterate $\hat{\boldsymbol{q}}^{(0)}$ be the solution to the uncoupled differential equation

$$\ddot{\hat{\boldsymbol{q}}}^{(0)} + 2\zeta\omega\dot{\hat{\boldsymbol{q}}}^{(0)} + \omega^2\hat{\boldsymbol{q}}^{(0)} = \boldsymbol{Q}(t, \boldsymbol{0}, \boldsymbol{0}) \qquad \hat{\boldsymbol{q}}^{(0)}(t_i) = \hat{\boldsymbol{q}}_i, \qquad \dot{\hat{\boldsymbol{q}}}^{(0)}(t_i) = \dot{\hat{\boldsymbol{q}}}_i \tag{9a}$$

obtained by Eq. (5). Define a recursive sequence $\{\hat{\boldsymbol{q}}^{(k)}\}$ of Picard iterates, where each successive iterate is the solution using Eq. (5) to the uncoupled equation with right-hand side forced by the previous iterate,

$$\ddot{\hat{\boldsymbol{q}}}^{(k)} + 2\zeta\omega\dot{\hat{\boldsymbol{q}}}^{(k)} + \omega^2\hat{\boldsymbol{q}}^{(k)} = \boldsymbol{Q}\big(t, \hat{\boldsymbol{q}}^{(k-1)}(t), \dot{\hat{\boldsymbol{q}}}^{(k-1)}(t)\big) - \boldsymbol{X}\dot{\hat{\boldsymbol{q}}}^{(k-1)}(t) \qquad \hat{\boldsymbol{q}}^{(k)}(t_i) = \hat{\boldsymbol{q}}_i, \qquad \dot{\hat{\boldsymbol{q}}}^{(k)}(t_i) = \dot{\hat{\boldsymbol{q}}}_i \tag{9b}$$

and where the forcing function is replaced by its piecewise linear approximation in time,

$$\hat{\boldsymbol{Q}}\big(t, \hat{\boldsymbol{q}}^{(k-1)}(t), \dot{\hat{\boldsymbol{q}}}^{(k-1)}(t)\big) = \boldsymbol{Q}\big(t_i, \hat{\boldsymbol{q}}^{(k-1)}(t_i), \dot{\hat{\boldsymbol{q}}}^{(k-1)}(t_i)\big)\frac{t_{i+1} - t}{t_{i+1} - t_i} + \boldsymbol{Q}\big(t_{i+1}, \hat{\boldsymbol{q}}^{(k-1)}(t_{i+1}), \dot{\hat{\boldsymbol{q}}}^{(k-1)}(t_{i+1})\big)\frac{t - t_i}{t_{i+1} - t_i} \tag{9c}$$

Computationally, the sequence of Picard iterates is considered to converge in modal acceleration norm to within a relative error tolerance of $\bar{\varepsilon}_2$ after $k$ iterations if $k$ is the smallest integer such that

$$\big\|\ddot{\hat{\boldsymbol{q}}}^{(k)}(t_{i+1}) - \ddot{\hat{\boldsymbol{q}}}^{(k-1)}(t_{i+1})\big\|_\infty \le \bar{\varepsilon}_2\big\|\ddot{\hat{\boldsymbol{q}}}^{(k)}(t_{i+1})\big\|_\infty \tag{10a}$$

Our computational experiments have indicated that the acceleration convergence test (10a) provides a slightly more reliable measure of convergence than do similar displacement and velocity tests.

Figure 3 demonstrates, for various numbers $n$ of time steps, the important computational property that Picard iteration is exponentially convergent, i.e.,

$$\big\|\ddot{\hat{\boldsymbol{q}}}^{(k)}(t_{i+1}) - \ddot{\hat{\boldsymbol{q}}}^{(k-1)}(t_{i+1})\big\|_\infty \le c_2 e^{-\mu k}\big\|\ddot{\hat{\boldsymbol{q}}}^{(k)}(t_{i+1})\big\|_\infty \tag{10b}$$

where $c_2$ and $\mu$ are constants depending upon the problem at hand. Observe that the number of decimals of accuracy varies linearly

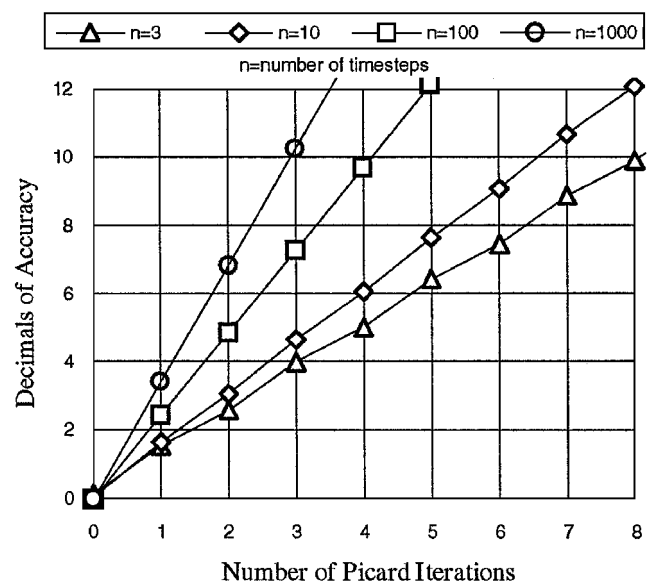


**Fig. 3 Exponential convergence of Picard iteration.**

with the number of iterations. If only a few decimals of accuracy are needed, the number of iterations can be kept small, and if greater accuracy is desired, a few more iterations will suffice. The convergence is seen to improve as the number $n$ of time steps increases. Convergence also has been found to improve as the level of damping increases. The example shown has a supercritically damped component, so that the zeroth iteration, which neglects off-diagonal damping terms entirely, is a poor approximation regardless of the number of time steps. Nevertheless, as the proof below shows, the convergence is always exponential for arbitrary choice of $\hat{q}^{(0)}$.

The test case from which Fig. 3 is taken has a forcing function that is piecewise linear. Consequently, the discretization error is zero by definition. The error due to the combined effects of discretization and Picard iteration can be bounded using the triangle inequality

$$\varepsilon_{\ddot{q}} = \left\|\ddot{q}(t) - \ddot{\hat{q}}^{(k)}(t)\right\|_\infty \le \|\ddot{q}(t) - \ddot{\hat{q}}(t)\|_\infty + \left\|\ddot{\hat{q}}(t) - \ddot{\hat{q}}^{(k)}(t)\right\|_\infty \le \left(\bar{\varepsilon}_1 + c_2 e^{-\mu k}\right)\|\ddot{q}(t)\|_\infty \tag{11a}$$

where $\bar{\varepsilon}_1$ bounds the relative discretization error and the term $c_2 e^{-\mu k}$ bounds the relative Picard iteration error. Thus, the total relative error may be expressed in terms of the number $n$ of time steps and the number $k$ of Picard iterations as

$$\bar{\varepsilon}_{\ddot{q}}(n,k) = \frac{\left\|\ddot{q}(t) - \ddot{\hat{q}}^{(k)}(t)\right\|_\infty}{\|\ddot{q}(t)\|_\infty} \le \frac{c_1}{n^2} + c_2 e^{-\mu k} \tag{11b}$$

In practice, Picard iteration error can be eliminated automatically relative to discretization error by simply setting the relative Picard tolerance to be somewhat less than the expected discretization error.

This section has presented several numerical test cases which suggest that Picard iteration converges exponentially to the exact solution of the coupled damping equations. These cases have only a few degrees of freedom. However, in a multihundred-degree-of-freedom commercial loads analysis[11] with coupled modal equations arising from aerodynamic stiffness and damping, the method of Picard iteration performed flawlessly, providing eight-place accuracy for several million integrations while never requiring more than six iterations. Our results indicate that, although the rate of convergence varies for different problems according to the number of time steps, the level of structural damping, whether aerodamping is present or not, etc., convergence has been exponential for all cases we have investigated and appears insensitive to the number of degrees of freedom. We will present a mathematical proof that convergence of Picard iteration (9) is always exponential under quite general conditions.

## V. Proof of Convergence of Picard Iteration

To prove the convergence of the Picard iterations in Eqs. (9), we convert the initial value problem (3) to an equivalent system of integral equations. The Picard iterations (9) are then equivalent to solving this system of integral equations by Picard iteration as well. Convergence follows as a consequence of the contraction mapping theorem in a form due to Bielecki.[12] The exponential convergence then is proved as a consequence of standard functional analytic error estimation techniques.

Observe that Eq. (3a) can be written as two first-order equations:

$$\begin{aligned} &\frac{\mathrm{d}}{\mathrm{d}t}\dot{\boldsymbol{q}} = -2\zeta\boldsymbol{\omega}\dot{\boldsymbol{q}} - \boldsymbol{\omega}^2\boldsymbol{q} + \boldsymbol{Q}(t,\boldsymbol{q},\dot{\boldsymbol{q}}) - \boldsymbol{X}\dot{\boldsymbol{q}} \\ &\frac{\mathrm{d}}{\mathrm{d}t}\boldsymbol{q} = \dot{\boldsymbol{q}}, \qquad \boldsymbol{q}(t_0) = \boldsymbol{q}_0, \qquad \dot{\boldsymbol{q}}(t_0) = \dot{\boldsymbol{q}}_0 \end{aligned} \tag{12}$$

which may be rewritten as a first-order equation in twice as many variables,

$$\dot{\boldsymbol{x}}(t) = \boldsymbol{A}\boldsymbol{x}(t) + \boldsymbol{F}(t,\boldsymbol{x}(t)), \qquad \boldsymbol{x}(t_0) = \boldsymbol{x}_0 \tag{13}$$

where

$$\boldsymbol{x} = \begin{Bmatrix}\dot{\boldsymbol{q}}\\ \boldsymbol{q}\end{Bmatrix}, \qquad A = \begin{bmatrix}-2\zeta\boldsymbol{\omega} & -\boldsymbol{\omega}^2\\ \boldsymbol{I} & \boldsymbol{0}\end{bmatrix}$$

$$\boldsymbol{F}(t,\boldsymbol{x}) = \begin{Bmatrix}\boldsymbol{Q}(t,\boldsymbol{q},\dot{\boldsymbol{q}}) - \boldsymbol{X}\dot{\boldsymbol{q}}\\ 0\end{Bmatrix}, \qquad \boldsymbol{x}_0 = \begin{Bmatrix}\dot{\boldsymbol{q}}_0\\ \boldsymbol{q}_0\end{Bmatrix} \tag{14}$$

Equation (13) may be multiplied by the integrating factor

$$e^{-t\boldsymbol{A}} = \sum_{j=0}^{\infty}\frac{(-t)^j}{j!}\boldsymbol{A}^j \tag{15}$$

where $e^{t\boldsymbol{A}}$ is the matrix exponential.[13] It follows by straightforward integration that

$$\boldsymbol{x}(t) = \exp[(t-t_0)\boldsymbol{A}]\boldsymbol{x}_0 + \int_{t_0}^{t}\exp[(t-s)\boldsymbol{A}]\boldsymbol{F}(s,\boldsymbol{x}(s))\,\mathrm{d}s \tag{16}$$

Therefore, the second-order initial value problem (3) is equivalent to a first-order initial value problem in the form (13) and hence is equivalent to an integral equation in the form (16).

The Picard iterations (9b) are equivalent to the iteration scheme

$$\boldsymbol{x}^{(k)}(t) = \exp[(t-t_0)\boldsymbol{A}]\boldsymbol{x}_0 + \int_{t_0}^{t}\exp[(t-s)\boldsymbol{A}]\boldsymbol{F}\left(s,\boldsymbol{x}^{(k-1)}(s)\right)\mathrm{d}s \tag{17}$$

and if $\boldsymbol{F}$ is replaced by $\hat{\boldsymbol{F}}$, the piecewise linear approximation to $\boldsymbol{F}$, we obtain the scheme (9b–c). We will prove that Eq. (17) solves Eq. (16) with arbitrary $\boldsymbol{x}^{(0)}(t)$. To do this, we need several definitions and results from analysis.

*Definition 1.* Let $(M, d)$ be a complete metric space with metric (distance) $d$. A mapping $T : M \to M$ is said to be contracting if there is a constant $\rho$, $0 \le \rho < 1$, called the contraction constant for $T$, such that

$$d(\boldsymbol{Tx}, \boldsymbol{Ty}) \le \rho\, d(\boldsymbol{x}, \boldsymbol{y}) \qquad \text{for all} \qquad \boldsymbol{x}, \boldsymbol{y} \in M \tag{18}$$

*Definition 2.* Let $\boldsymbol{T} : M \to M$. We say $\boldsymbol{T}$ has a fixed point $\boldsymbol{x} \in M$ if $\boldsymbol{Tx} = \boldsymbol{x}$.

*Theorem 1 (contraction mapping theorem).* (A proof can be found in Ref. 14.) Let $(M, d)$ be a complete metric space and let $\boldsymbol{T} : M \to M$ be a contraction mapping. Then $\boldsymbol{T}$ has a unique fixed point $\boldsymbol{x} \in M$. Moreover, $\boldsymbol{x} = \lim_{k\to\infty}\boldsymbol{x}^{(k)}$, where $\{\boldsymbol{x}^{(k)}\}$ is defined recursively by $\boldsymbol{x}^{(k)} = \boldsymbol{T}\boldsymbol{x}^{(k-1)}$ with $\boldsymbol{x}^{(0)}$ an arbitrary element in $M$. In addition, we have the error estimate

$$d\left(\boldsymbol{x}, \boldsymbol{x}^{(k)}\right) \le \frac{\rho^k d\left(\boldsymbol{x}, \boldsymbol{T}\boldsymbol{x}^{(0)}\right)}{1-\rho} \tag{19}$$

Note that, for $0 < \rho < 1$, we can write $\rho = e^{-\mu}$ for some $\mu > 0$, so that Eq. (19) becomes

$$d\left(\boldsymbol{x}, \boldsymbol{x}^{(k)}\right) \le \frac{e^{-\mu k} d\left(\boldsymbol{x}, \boldsymbol{T}\boldsymbol{x}^{(0)}\right)}{1-\rho} \tag{20}$$

which will show that the Picard iterations $\{\boldsymbol{x}^{(k)}\}$ converge exponentially to $\boldsymbol{x}$.

To apply Theorem 1 to Eq. (19), we need to show that the mapping

$$\boldsymbol{Tx}(t) = \exp[(t-t_0)\boldsymbol{A}]\boldsymbol{x}_0 + \int_{t_0}^{t}\exp[(t-s)\boldsymbol{A}]\boldsymbol{F}(s,\boldsymbol{x}(s))\,\mathrm{d}s \tag{21}$$

defines a contraction mapping on a suitable complete metric space. First, some additional theorems and definitions are needed.

*Theorem 2.* Let $[a, b]$ be a bounded interval on the real line $\mathfrak{R}$ and let $C[a, b] \equiv C$ be the space of continuous functions on $[a, b]$. Let $f$ and $g$ belong to $C$. Define a metric $d_\lambda$, where $-\infty < \lambda < \infty$, by

$$d_\lambda(f, g) = \max_{a\le t\le b}|\exp[-\lambda(t-a)](f(t) - g(t))| \equiv \|f - g\|_{(\lambda)} \tag{22}$$

Then $(C, d_\lambda)$ is a complete metric space. The proof can be found in Ref. 12. Note that if $\lambda = 0$, then $\|f - g\|_{(0)} \equiv \|f - g\|_\infty$, which is called the uniform distance on $C$. It is shown easily that convergence with respect to $d_\lambda$ is equivalent to uniform convergence.

Theorem 2 can be extended to vector-valued functions in the following way: Let $\boldsymbol{f}(t) = (f_1(t), \ldots, f_m(t))$ and define

$$d_\lambda(\boldsymbol{f}, \boldsymbol{g}) \equiv \|\boldsymbol{f} - \boldsymbol{g}\|_\lambda = \max_{1\le i\le m}\|f_i - g_i\|_\lambda \tag{23}$$

If $C^{(m)}$ is the space of continuous vector-valued functions on $[a, b]$, then $(C^{(m)}, d_\lambda)$ is a complete metric space.[12] Similarly, for $m = 1$, convergence in $C_\lambda^{(m)}$ is equivalent to uniform convergence, i.e., convergence in $C_0^{(m)}$.

By suitably choosing $\lambda$ and for appropriate conditions on $\boldsymbol{F}$, we can show that $\boldsymbol{T}$ given by Eq. (21) is a contraction mapping and the exponential convergence of the Picard iterations (9) will follow from Theorem 1.

*Definition 3.* Let $\boldsymbol{f}(t, \boldsymbol{x}) : [a, b] \times \mathfrak{R}^m \to \mathfrak{R}^m$ be a continuous function in $(t, \boldsymbol{x})$. We say that $\boldsymbol{f}(t, \boldsymbol{x})$ is Lipschitz continuous in $\boldsymbol{x}$ if there is a positive and continuous (hence bounded) function $\alpha$ on $[a, b]$ such that

$$|\boldsymbol{f}(t, \boldsymbol{x}) - \boldsymbol{f}(t, \boldsymbol{y})| \le \alpha(t) \max_{1 \le i \le m} |x_i - y_i| \tag{24}$$

Now let $\boldsymbol{F}(t, \boldsymbol{x})$ in Eq. (16) be Lipschitz continuous in $\boldsymbol{x}$. Then there is a positive and continuous function $\beta(t)$ on $[a, b]$ such that

$$\|\boldsymbol{F}(t, \boldsymbol{x}) - \boldsymbol{F}(t, \boldsymbol{y})\|_\infty \le \beta(t) \|\boldsymbol{x} - \boldsymbol{y}\|_\infty \tag{25}$$

*Lemma 1.* If $\boldsymbol{A} = [a_{ij}]$ is an $m \times m$ matrix, define the matrix norm of $\boldsymbol{A}$ by $\|\boldsymbol{A}\| \equiv \max_{1 \le i, j \le m} |a_{ij}|$. Then: (i) $\|\boldsymbol{A}\boldsymbol{x}\|_\infty \le \|\boldsymbol{A}\| \|\boldsymbol{x}\|_\infty$; (ii) $\|\boldsymbol{A}^k\| \le \|\boldsymbol{A}\|^k$ for $k \ge 1$; (iii) $\|e^{t\boldsymbol{A}}\| \le e^{t\|\boldsymbol{A}\|}$; and (iv) $\|e^{t\boldsymbol{A}}\boldsymbol{x}\|_\infty \le e^{t\|\boldsymbol{A}\|} \|\boldsymbol{x}\|_\infty$.

*Proof.* Properties (i–iii) follow by straightforward computation using Eq. (23) with $\lambda = 0$ and Eq. (15); (iv) then follows from (i) and (iii).

*Lemma 2.* If $t_0 \le t \le t_n$ and $\boldsymbol{F}(t, \boldsymbol{x})$ in Eq. (16) is Lipschitz continuous, then $\boldsymbol{T} : C_\lambda^{(m)} \to C_\lambda^{(m)}$ given by Eq. (21) is well defined, and if $\lambda$ is chosen so that

$$\lambda > D \equiv \max_{(t,s) \in [t_0, t_n] \times [t_0, t_n]} \beta(s) \exp[(t - s)\|\boldsymbol{A}\|] \tag{26}$$

where $\beta$ is the Lipschitz coefficient in Eq. (25), then $\boldsymbol{T}$ is contracting.

*Proof.* To show that $\boldsymbol{T}$ is well defined on $C_\lambda^{(m)}$, we appeal to a standard result that, if $\boldsymbol{x}$ is continuous, then $\boldsymbol{T}\boldsymbol{x}$ is continuous.[12] To prove that $\boldsymbol{T}$ is contracting, we calculate

$$\begin{aligned} &|\exp[-\lambda(t - t_0)][\boldsymbol{T}\boldsymbol{x}(t) - \boldsymbol{T}\boldsymbol{y}(t)]_i| \\ &\quad = \exp[-\lambda(t - t_0)] \left| \int_{t_0}^{t} \exp[\lambda(s - t_0)] g_i(s)\, ds \right| \end{aligned} \tag{27}$$

where

$$\boldsymbol{g}(s) = \exp[-\lambda(s - t_0)] \exp[(t - s)\boldsymbol{A}](\boldsymbol{F}(s, \boldsymbol{x}) - \boldsymbol{F}(s, \boldsymbol{y}))$$

and where $[\,]_i$ denotes the $i$th component of the corresponding vector. From the integral form of the triangle inequality, we obtain

$$\left| \int_{t_0}^{t} \exp[\lambda(s - t_0)] g_i(s)\, ds \right| \le \int_{t_0}^{t} \exp[\lambda(s - t_0)] |g_i(s)|\, ds \tag{28}$$

and from the definition of the infinity norm,

$$|g_i(s)| \le \|\boldsymbol{g}(s)\|_\infty = \|\exp[(t - s)\boldsymbol{A}]\boldsymbol{h}(s)\|_\infty$$

where

$$\boldsymbol{h}(s) = [\boldsymbol{F}(s, \boldsymbol{x}) - \boldsymbol{F}(s, \boldsymbol{y})] \exp[-\lambda(s - t_0)]$$

From Lemma 1(iv),

$$\|\exp[(t - s)\boldsymbol{A}]\boldsymbol{h}(s)\|_\infty \le \exp[(t - s)\|\boldsymbol{A}\|] \|\boldsymbol{h}(s)\|_\infty$$

Using the Lipschitz continuity of $\boldsymbol{F}$ and Eq. (25),

$$\|\boldsymbol{h}(s)\|_\infty \le \beta(s) \exp[-\lambda(s - t_0)] \|\boldsymbol{x}(s) - \boldsymbol{y}(s)\|_\infty$$

Hence, the integral in Eq. (28) is bounded by

$$\int_{t_0}^{t} \beta(s) \exp[(t - s)\|\boldsymbol{A}\|] \|\boldsymbol{x}(s) - \boldsymbol{y}(s)\|_\infty\, ds \tag{29}$$

Using Eq. (29) and the definition of $D$ in Eq. (26), the right-hand side of Eq. (27) is bounded by

$$\begin{aligned} &\exp[-\lambda(t - t_0)] D \|\boldsymbol{x} - \boldsymbol{y}\|_{(\lambda)} \int_{t_0}^{t} \exp[\lambda(s - t_0)]\, ds \\ &\quad = \frac{D}{\lambda} \{1 - \exp[-\lambda(t - t_0)]\} \|\boldsymbol{x} - \boldsymbol{y}\|_{(\lambda)} \end{aligned} \tag{30}$$

Thus,

$$\|\boldsymbol{T}\boldsymbol{x} - \boldsymbol{T}\boldsymbol{y}\|_{(\lambda)} \le \rho \|\boldsymbol{x} - \boldsymbol{y}\|_{(\lambda)} \tag{31}$$

where $\rho = D/\lambda < 1$ because in Eq. (26) we chose $\lambda > D$. Hence, $\boldsymbol{T}$ is contracting on $C_\lambda^{(m)}$.

*Theorem 3.* In Eq. (16), assume that $\boldsymbol{F}$ is Lipschitz continuous. Then, the Picard iterations (17) converge uniformly and exponentially to the unique solution of the integral equation (16).

*Proof.* It follows from the contraction mapping theorem and Lemma 2 that the Picard approximations converge to the unique solution to Eq. (16). Because convergence with respect to $d_\lambda$ is equivalent to uniform convergence, the Picard iterations $\{\boldsymbol{x}^{(k)}\}$ converge uniformly to $\boldsymbol{x}$. The exponential convergence follows from Eq. (20).

*Theorem 4.* Assume that the generalized forces $\boldsymbol{Q}$ in Eq. (3) are Lipschitz continuous (in particular if they are linear). Then, the Picard iterations $\boldsymbol{q}^{(k)}$ and $\dot{\boldsymbol{q}}^{(k)}$ converge uniformly and exponentially to $\boldsymbol{q}$ and $\dot{\boldsymbol{q}}$.

*Proof.* This follows immediately from Theorem 3 and our previous remarks concerning the equivalence of Eqs. (3) and (16).

*Corollary 1.* Under the conditions of Theorem 4, the Picard iterations $\ddot{\boldsymbol{q}}^{(k)}$ converge uniformly and exponentially to $\ddot{\boldsymbol{q}}$.

*Proof.* From Eq. (9) and the definition of Picard iteration we have

$$\ddot{\boldsymbol{q}}^{(k)} = -(2\zeta\boldsymbol{\omega} + \boldsymbol{X})\dot{\boldsymbol{q}}^{(k)} - \boldsymbol{\omega}^2 \boldsymbol{q}^{(k)} + \boldsymbol{Q}\big(t, \boldsymbol{q}^{(k-1)}, \dot{\boldsymbol{q}}^{(k-1)}\big) \tag{32}$$

and

$$\ddot{\boldsymbol{q}} = -(2\zeta\boldsymbol{\omega} + \boldsymbol{X})\dot{\boldsymbol{q}} - \boldsymbol{\omega}^2 \boldsymbol{q} + \boldsymbol{Q}(t, \boldsymbol{q}, \dot{\boldsymbol{q}}) \tag{33}$$

Subtracting Eq. (32) from Eq. (33) gives

$$\begin{aligned} \ddot{\boldsymbol{q}} - \ddot{\boldsymbol{q}}^{(k)} &= -(2\zeta\boldsymbol{\omega} + \boldsymbol{X})\big(\dot{\boldsymbol{q}} - \dot{\boldsymbol{q}}^{(k)}\big) - \boldsymbol{\omega}^2\big(\boldsymbol{q} - \boldsymbol{q}^{(k)}\big) \\ &\quad + \big(\boldsymbol{Q}(t, \boldsymbol{q}, \dot{\boldsymbol{q}}) - \boldsymbol{Q}\big(t, \boldsymbol{q}^{(k-1)}, \dot{\boldsymbol{q}}^{(k-1)}\big)\big) \end{aligned} \tag{34}$$

Using the Lipschitz continuity of $\boldsymbol{Q}$ and the exponential convergence of $\boldsymbol{q}^{(k)}$ and $\dot{\boldsymbol{q}}^{(k)}$, it follows from Lemma 1(iii) that $\ddot{\boldsymbol{q}}^{(k)}$ converges exponentially to $\ddot{\boldsymbol{q}}$.

*Corollary 2.* The Picard iterations in Eqs. (9) using the piecewise linear approximation $\hat{\boldsymbol{Q}}$ to $\boldsymbol{Q}$ converge uniformly and exponentially to $\hat{\boldsymbol{q}}$.

*Proof.* Because $\boldsymbol{Q}$ is Lipschitz continuous, it follows from Eq. (9c) that $\hat{\boldsymbol{Q}}$ is also Lipschitz continuous. Hence, the convergence of $\boldsymbol{q}^{(k)}$, $\dot{\boldsymbol{q}}^{(k)}$, and $\ddot{\boldsymbol{q}}^{(k)}$ follows from Theorem 4 and Corollary 1.

If we impose some additional conditions on $\boldsymbol{Q}$, we can establish the error estimate (11b) for the convergence of the Picard iterations $\hat{\boldsymbol{q}}^{(k)}$, $\hat{\dot{\boldsymbol{q}}}^{(k)}$, and $\hat{\ddot{\boldsymbol{q}}}^{(k)}$ to $\boldsymbol{q}$, $\dot{\boldsymbol{q}}$, and $\ddot{\boldsymbol{q}}$.

*Theorem 5.* Assume that, in addition to being Lipschitz continuous, the generalized forces are twice continuously differentiable in $(\boldsymbol{q}, \dot{\boldsymbol{q}})$ with uniformly bounded second partial derivatives. Then

$$\big\|\boldsymbol{q} - \hat{\boldsymbol{q}}^{(k)}\big\|_\infty \le \big(c_1/n^2\big) + c_2 e^{-\mu k} \tag{35}$$

with similar bounds for $\|\dot{\boldsymbol{q}} - \hat{\dot{\boldsymbol{q}}}^{(k)}\|_\infty$ and $\|\ddot{\boldsymbol{q}} - \hat{\ddot{\boldsymbol{q}}}^{(k)}\|_\infty$.

*Proof.* To prove bounds for $\|\boldsymbol{q} - \boldsymbol{q}^{(k)}\|_\infty$ and $\|\dot{\boldsymbol{q}} - \dot{\boldsymbol{q}}^{(k)}\|_\infty$, we use the equivalent Picard iterations for Eq. (17). The bounds for $\hat{\boldsymbol{q}}$ then are established as in Corollary 2. Let $\hat{\boldsymbol{x}}^{(k)}$ denote the Picard iterations in Eq. (17) with $\boldsymbol{F}$ replaced by $\hat{\boldsymbol{F}}$, the piecewise linear approximation to $\boldsymbol{F}$. By the triangle inequality,

$$\big\|\boldsymbol{x} - \hat{\boldsymbol{x}}^{(k)}\big\|_\infty \le \big\|\boldsymbol{x} - \boldsymbol{x}^{(k)}\big\|_\infty + \big\|\boldsymbol{x}^{(k)} - \hat{\boldsymbol{x}}^{(k)}\big\|_\infty \tag{36}$$

From Theorem 3, it follows that $\|\boldsymbol{x} - \boldsymbol{x}^{(k)}\|_\infty \leq c_2 \exp(-\mu k)$ for some $c_2$ and $\mu > 0$. Hence, it remains to bound $\|\boldsymbol{x}^{(k)} - \hat{\boldsymbol{x}}^{(k)}\|_\infty$. From Eq. (17) with $\boldsymbol{F}$ and $\hat{\boldsymbol{F}}$,

$$\boldsymbol{x}^{(k)}(t) = \exp[(t-t_0)\boldsymbol{A}]\boldsymbol{x}_0 + \int_{t_0}^{t} \exp[(t-s)\boldsymbol{A}]F\big(s, \boldsymbol{x}^{(k-1)}(s)\big)\,\mathrm{d}s \tag{37}$$

$$\hat{\boldsymbol{x}}^{(k)}(t) = \exp[(t-t_0)\boldsymbol{A}]\hat{\boldsymbol{x}}_0 + \int_{t_0}^{t} \exp[(t-s)\boldsymbol{A}]\hat{F}\big(s, \hat{\boldsymbol{x}}^{(k-1)}(s)\big)\,\mathrm{d}s \tag{38}$$

Subtracting Eq. (38) from Eq. (37) gives

$$\boldsymbol{x}^{(k)}(t) - \hat{\boldsymbol{x}}^{(k)}(t) = \exp[(t-t_0)\boldsymbol{A}][\boldsymbol{x}_0 - \hat{\boldsymbol{x}}_0] + \int_{t_0}^{t} \exp[(t-s)\boldsymbol{A}] \times \Big[\boldsymbol{F}\big(s, \boldsymbol{x}^{(k-1)}(s)\big) - \hat{\boldsymbol{F}}\big(s, \hat{\boldsymbol{x}}^{(k-1)}(s)\big)\Big]\,\mathrm{d}s \tag{39}$$

For simplicity, we assume as in Lemma 2 that $\boldsymbol{x}_0 = \hat{\boldsymbol{x}}_0$ and, arguing as in Lemma 2, we find that

$$\big\|\boldsymbol{x}^{(k)} - \hat{\boldsymbol{x}}^{(k)}\big\|_\infty \leq c \int_{t_0}^{t} \big\|\boldsymbol{F}\big(s, \boldsymbol{x}^{(k-1)}(s)\big) - \hat{\boldsymbol{F}}\big(s, \hat{\boldsymbol{x}}^{(k-1)}(s)\big)\big\|_\infty\,\mathrm{d}s \tag{40}$$

To bound $\|\boldsymbol{F}(s, \boldsymbol{x}^{(k-1)}(s)) - \hat{\boldsymbol{F}}(s, \hat{\boldsymbol{x}}^{(k-1)}(s))\|_\infty$, we need the following result from interpolation theory. Let $\boldsymbol{f}(t)$ be a twice continuously differentiable function on an interval $[a, b]$. Let $\hat{\boldsymbol{f}}$ be the piecewise linear interpolant to $\boldsymbol{f}$ relative to the partition $[a, b] = [a, a+h, a+2h, \ldots, b]$, $h = (b-a)/n$. Then

$$\|\boldsymbol{f} - \hat{\boldsymbol{f}}\|_\infty \leq \frac{c_1 \|\ddot{\boldsymbol{f}}\|_\infty}{n^2} \tag{41}$$

Thus, from Eq. (40) and the assumed properties of $\boldsymbol{F}$, it follows that

$$\big\|\boldsymbol{F}\big(s, \boldsymbol{x}^{(k-1)}(s)\big) - \hat{\boldsymbol{F}}\big(s, \hat{\boldsymbol{x}}^{(k-1)}(s)\big)\big\|_\infty \leq \big(c_1/n^2\big) \tag{42}$$

where $c_1$ depends on second partial derivatives of $\boldsymbol{F}(s, \boldsymbol{x})$ in $\boldsymbol{x}$, which by assumption are uniformly bounded. This completes the proof that the modally coupled equations of motion (3) can be integrated to arbitrary accuracy using Picard iteration in the form (9).

## VI. Solution of Thomson's Problem

The well-known text by Thomson[15] discusses a simple two-degree-of-freedom system with modally coupled damping but offers no solution. Thomson's problem is depicted in Fig. 4. It consists of two equal masses connected together and grounded by three equal springs. The masses also are connected by a viscous damper and one of them is grounded with an equal damper. The grounded damper results in the modal damping matrix being coupled. Both masses are excited from rest by sinusoidal forcing functions. Referring to Fig. 4, the equations of motion are immediately seen to be

$$\begin{bmatrix} m & 0 \\ 0 & m \end{bmatrix}\begin{Bmatrix} \ddot{u}_1 \\ \ddot{u}_2 \end{Bmatrix} + \begin{bmatrix} 2c & -c \\ -c & c \end{bmatrix}\begin{Bmatrix} \dot{u}_1 \\ \dot{u}_2 \end{Bmatrix} + \begin{bmatrix} 2k & -k \\ -k & 2k \end{bmatrix}\begin{Bmatrix} u_1 \\ u_2 \end{Bmatrix} = \begin{Bmatrix} F_1 \sin \omega t \\ F_2 \sin \omega t \end{Bmatrix} \begin{Bmatrix} u_1(0) \\ u_2(0) \end{Bmatrix} = \begin{Bmatrix} 0 \\ 0 \end{Bmatrix}, \begin{Bmatrix} \dot{u}_1(0) \\ \dot{u}_2(0) \end{Bmatrix} = \begin{Bmatrix} 0 \\ 0 \end{Bmatrix} \tag{43}$$

For the purpose of this example, let $m = 1$ lb·s$^2$/in. (175.126 kg), $k = 4\pi^2$ lb/in. (6913.70 N/m), and $c = 4\pi$ lb·s$^2$/in. (2200.70 N·s/m). This tunes the system to $f_1 = 1$ Hz and $f_2 = \sqrt{3}$ Hz, and causes the modal damping ratios to be $\zeta_1 = 0.5$ and $\zeta_2 = 2.5/\sqrt{3}$ so that one mode is subcritically damped and the other is supercritically damped. The modal matrix and modal damping matrix are easily found to be

$$\boldsymbol{\Phi} = \begin{bmatrix} 1/\sqrt{2} & 1/\sqrt{2} \\ 1/\sqrt{2} & -1/\sqrt{2} \end{bmatrix}, \qquad \boldsymbol{\Phi}^T \boldsymbol{C} \boldsymbol{\Phi} = \begin{bmatrix} 2\pi & 2\pi \\ 2\pi & 10\pi \end{bmatrix} \tag{44}$$

However, if the off-diagonal terms of the modal damping matrix are ignored, then the resulting false damping matrix,

$$\boldsymbol{C}_{\text{false}} = (\boldsymbol{\Phi}^T)^{-1}\,\mathrm{diag}(\boldsymbol{\Phi}^T \boldsymbol{C} \boldsymbol{\Phi})(\boldsymbol{\Phi})^{-1} = \begin{bmatrix} 3c/2 & -c \\ -c & 3c/2 \end{bmatrix} \neq \boldsymbol{C} = \begin{bmatrix} 2c & -c \\ -c & c \end{bmatrix} \tag{45}$$

is seen to be equivalent to reducing the original grounding damper on the left wall by half and placing a second grounding damper symmetrically on the right wall, obviously representing a different mechanical system.

Consider first the physical response when the external forces act in phase with one another. In the original system, $u_2$ will respond more than $u_1$ because of the grounding damper acting on $u_1$. However, in the false system, the two masses will respond equally because of the falsely imposed symmetry. When the forces act out of phase, then in the original system, $u_2$ will again respond more than $u_1$ but they will start off out of phase. However, in the false system, $u_1$ and $u_2$ will have exactly the same magnitude and will always be 180 deg out of phase. Figure 5 compares the solution to Thomson's problem computed three different ways with $F_1 = \pm F_2 = 10$ lb (44.482 N) at a frequency of 1.5 hz. Results from the methods of Picard iteration (9) and linear modal velocity (6) are plotted in bold and overlay one another (to nine decimal places). Results from neglecting modal coupling, plotted with a lightweight line, overpredict $u_1$ by 65.48% out of phase and 7.73% in phase, underpredict $u_2$ by 57.51% out of phase and 30.19% in phase, and have significant phase errors for the out-of-phase excitation. Thus, loads computed by neglecting coupled modal damping can be seriously in error.

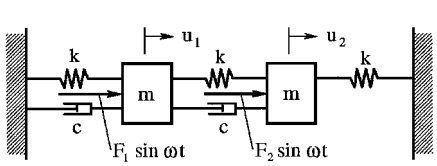


**Fig. 4 Thomson's problem.**

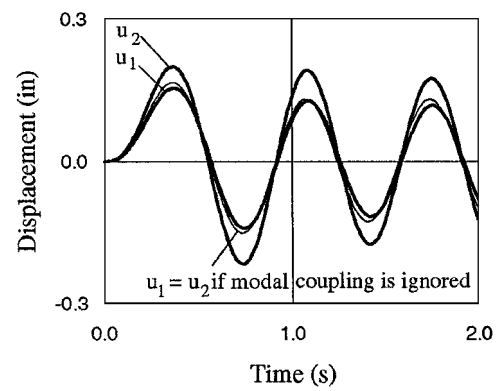


**a) In-phase excitation**

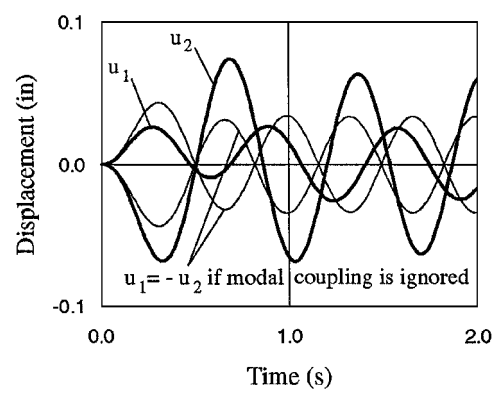


**b) Out-of-phase excitation**

**Fig. 5 Solution of Thomson's problem.**

Thomson's two-degree-of-freedom problem not only provides an elementary example of a modally coupled system but also demonstrates the important property of multiple-degree-of-freedom systems that ignoring the effects of modal coupling can overpredict loads generally and also may underpredict some loads. This is consistent with previous results for large complex aerospace structures.[2,3,6]

## VII. Conclusions

We have shown that the quasilinear second-order matrix differential equations of structural dynamics, including the effects of general structural damping, aerodynamic damping and stiffness, and nonlinear forcing functions, can be integrated quickly and accurately by Picard iteration in the form (9) by Dawson. For the special case of general structural damping with forcing functions that depend only on time and with no aerodynamic forces, Picard iteration and the linear modal velocity method (6) developed by Henkel and Mar and others agree to within machine accuracy. The proof that Picard iteration is exact to within discretization error for the general case computationally proves the correctness of the latter in the special case. This confirms their earlier assertion that their method is mathematically exact except for discretization error.[3,6,9]

The method of Picard iteration is intuitive, powerful, easy to program, fast, accurate, and unconditionally stable. Existing computer programs using the standard piecewise linear closed-form solution (5) for solving modally uncoupled problems can be modified easily to perform Picard iteration. Also, Picard iteration can be stopped after the zeroth iteration should it be desired to neglect modal coupling.

Several areas of future research may be of interest. The mathematical condition used in the proof of convergence that the generalized forces be Lipschitz continuous is sufficient but not necessary. Therefore a tighter proof might be found. Forcing functions involving friction that depend upon the direction of impending motion, or contact and release discontinuities such as can occur during liftoff, landing, or docking, are not globally Lipschitz continuous, but they are Lipschitz continuous between discontinuities. Thus, application of Picard iteration to problems involving friction and rheonomous constraints would appear promising. For spacecraft isolation systems with nonlinear struts or other structures with nonlinear stiffness and damping properties, Picard iteration can be applied by transferring incremental nonlinearities to the right-hand side.

## Acknowledgments

The authors acknowledge Robert E. Dawson for first applying the method of Picard iteration to coupled loads analysis of spacecraft and space launch vehicles with coupled modal damping, and to Edwin E. Henkel, J. Michael Chapman, Ayman Abdallah, and others for helpful discussions during the writing of this paper.

## References

[1]Craig, R. R., *Structural Dynamics*, Wiley, New York, 1981, Chap. 17.

[2]Fromme, J. A., and Stroman, M. M., "Titan IV Indicator Payload Technique: Motivation, Theory and Results," Lockheed Martin Astronautics, MCR 92-8224, Denver, CO, Sept. 1992.

[3]Henkel, E. E., and Mar, R., "Transient Solution of Coupled Structural Components Using System Modal Coordinates with and Without Coupled System Damping," *Proceedings of Damping '93 Conference*, 1993.

[4]Balmès, E., and Crawley, E. F. (advisor), "Experimental/Analytical Predictive Models of Damped Structural Dynamics," MIT Space Engineering Research Center Rept. 7-93, based on Ph.D. Dissertation, Dept. of Aeronautics and Astronautics, Massachusetts Inst. of Technology, Cambridge, MA, 1993.

[5]Foss, K. A., "Co-Ordinates Which Uncouple the Equations of Motion of Damped Linear Dynamic Systems," *Proceedings of ASME Annual Meeting*, American Society of Mechanical Engineers, New York, 1957 (Paper 57-A-86).

[6]Chapman, J. M., "Incorporating a Full Damping Matrix in the Transient Analyses of Nonlinear Structures," *Proceedings of Damping '93 Conference*, 1993.

[7]Dawson, R. E., "Coupled Damping Transient Response Methodology," Lockheed Martin Astronautics, Letter SLS-92-20381, Enclosure 1, Denver, CO, Sept. 1992.

[8]Davies, B., *Integral Transforms and Their Applications*, Vol. 25, Applied Mathematics Series, Springer–Verlag, New York, 1978.

[9]Fromme, J. A., "Automatic Loads Cycle Program ***alc***: Rapid Structural Dynamics Loads Analysis," Astrodyne Research and Development, TR 96-1, Morrison, CO, June 1996.

[10]Fromme, J. A., "Nonlinear (and Linear) Viscoelastic Space Truss Analysis," Astrodyne Research and Development, ITN 8A, Morrison, CO, Jul. 1994.

[11]Fromme, J. A., "Long March 2C/SD Maximum Airloads Independent Verification and Validation: Spacecraft and Payload Fairing Loads," Astrodyne Research and Development, Contract C456JE Final Rept., Morrison, CO, Jan. 1996.

[12]Bielecki, A., "Une remarque sur la Méthode de Banach-Cacciopoli-Tikhonov dan la Théorie des Équationes Différéntielles Ordinaires," Bulletin de l'Academie Polonaise des Sciences, Serie des Sciences, Mathematiques, Astronomiques et Physiques, Vol. 4, 1956, pp. 261–264.

[13]Strang, G., *Linear Algebra and Its Applications*, Academic, New York, 1976, p. 197.

[14]Golberg, M. A., and Chen, C. S., *Discrete Projection Methods for Integral Equations*, Computational Mechanics Publications, Southampton, England, UK, 1997, Chap. 4.

[15]Thomson, W. T., *Theory of Vibration with Applications*, Prentice–Hall, Englewood Cliffs, NJ, 1972, pp. 183–187.

A. Berman
*Associate Editor*